Biomedical Optics EXPRESS

# Rapid imaging of surgical breast excisions using direct temporal sampling two photon fluorescent lifetime imaging

**Michael G. Giacomelli,[1] Yuri Sheikine,[2,3] Hilde Vardeh,[2] James L. Connolly,[2] and James G. Fujimoto[1,*]**

[1]*Department of Electrical Engineering and Computer Science and Research Laboratory of Electronics, Massachusetts Institute of Technology, Cambridge, MA, USA*
[2]*Department of Pathology, Beth Israel Deaconess Medical Center, Harvard Medical School, Boston, MA 02215, USA*
[3]*Alternative spelling of this author's name is Yury Sheykin*
[*]*jgfuji@mit.edu*

**Abstract:** Two photon fluorescent lifetime imaging is a modality that enables depth-sectioned, molecularly-specific imaging of cells and tissue using intrinsic contrast. However, clinical applications have not been well explored due to low imaging speed and limited field of view, which make evaluating large pathology samples extremely challenging. To address these limitations, we have developed direct temporal sampling two photon fluorescent lifetime imaging (DTS-FLIM), a method which enables a several order of magnitude increase in imaging speed by capturing an entire lifetime decay in a single fluorescent excitation. We use this greatly increased speed to perform a preliminary study using gigapixel-scale imaging of human breast pathology surgical specimens.



**OCIS codes:** (170.2520) Fluorescence microscopy; (170.3880) Medical and biological imaging.

## References and links

1. "Cancer Facts and Figures," (American Cancer Society, 2014).
2. J. D. Bancroft and A. Stevens, *Theory and Practice of Histological Techniques,* 6th ed. (Churchill Livingstone, Edinburgh; New York, 2008), pp. xiv, 726.
3. J. M. Uecker, E. H. Bui, K. H. Foulkrod, and J. P. Sabra, "Intraoperative assessment of breast cancer specimens decreases cost and number of reoperations," Am. Surg. **77**(3), 342–344 (2011).
4. J. A. van Dongen, A. C. Voogd, I. S. Fentiman, C. Legrand, R. J. Sylvester, D. Tong, E. van der Schueren, P. A. Helle, K. van Zijl, and H. Bartelink, "Long-term results of a randomized trial comparing breast-conserving therapy with mastectomy: European Organization for Research and Treatment of Cancer 10801 trial," J. Natl. Cancer Inst. **92**(14), 1143–1150 (2000).
5. J. Engel, J. Kerr, A. Schlesinger-Raab, H. Sauer, and D. Hölzel, "Quality of life following breast-conserving therapy or mastectomy: results of a 5-year prospective study," Breast J. **10**(3), 223–231 (2004).
6. F. J. Fleming, A. D. Hill, E. W. Mc Dermott, A. O'Doherty, N. J. O'Higgins, and C. M. Quinn, "Intraoperative margin assessment and re-excision rate in breast conserving surgery," Eur. J. Surg. Oncol. **30**(3), 233–237 (2004).
7. G. P. Swanson, K. Rynearson, and R. Symmonds, "Significance of margins of excision on breast cancer recurrence," Am. J. Clin. Oncol. **25**(5), 438–441 (2002).
8. K. Esbona, Z. Li, and L. G. Wilke, "Intraoperative Imprint Cytology and Frozen Section Pathology for Margin Assessment in Breast Conservation Surgery: A Systematic Review," Ann. Surg. Oncol. **19**(10), 3236–3245 (2012).
9. F. Helmchen and W. Denk, "Deep tissue two-photon microscopy," Nat. Methods **2**(12), 932–940 (2005).
10. W. R. Zipfel, R. M. Williams, R. Christie, A. Y. Nikitin, B. T. Hyman, and W. W. Webb, "Live tissue intrinsic emission microscopy using multiphoton-excited native fluorescence and second harmonic generation," Proc. Natl. Acad. Sci. U.S.A. **100**(12), 7075–7080 (2003).
11. S. J. Schnitt, "The diagnosis and management of pre-invasive breast disease: flat epithelial atypia--classification, pathologic features and clinical significance," Breast Cancer Res. **5**(5), 263–268 (2003).
12. P. P. Provenzano, K. W. Eliceiri, J. M. Campbell, D. R. Inman, J. G. White, and P. J. Keely, "Collagen reorganization at the tumor-stromal interface facilitates local invasion," BMC Med. **4**(1), 38 (2006).

#247756 Received 11 Aug 2015; revised 1 Oct 2015; accepted 1 Oct 2015; published 8 Oct 2015

13. Y. K. Tao, D. Shen, Y. Sheikine, O. O. Ahsen, H. H. Wang, D. B. Schmolze, N. B. Johnson, J. S. Brooker, A. E. Cable, J. L. Connolly, and J. G. Fujimoto, "Assessment of breast pathologies using nonlinear microscopy," Proc. Natl. Acad. Sci. U.S.A. **111**(43), 15304–15309 (2014).
14. P. T. C. So, T. French, W. M. Yu, K. M. Berland, C. Y. Dong, and E. Gratton, "Time-resolved fluorescence microscopy using two-photon excitation," Bioimaging **3**(2), 49–63 (1995).
15. M. C. Skala, K. M. Riching, D. K. Bird, A. Gendron-Fitzpatrick, J. Eickhoff, K. W. Eliceiri, P. J. Keely, and N. Ramanujam, "In vivo multiphoton fluorescence lifetime imaging of protein-bound and free nicotinamide adenine dinucleotide in normal and precancerous epithelia," J. Biomed. Opt. **12**(2), 024014 (2007).
16. H.-J. Lin, P. Herman, and J. R. Lakowicz, "Fluorescence lifetime-resolved pH imaging of living cells," Cytometry A **52**(2), 77–89 (2003).
17. K. Okabe, N. Inada, C. Gota, Y. Harada, T. Funatsu, and S. Uchiyama, "Intracellular temperature mapping with a fluorescent polymeric thermometer and fluorescence lifetime imaging microscopy," Nat. Commun. **3**, 705 (2012).
18. V. K. Ramanujan, J.-H. Zhang, E. Biener, and B. Herman, "Multiphoton fluorescence lifetime contrast in deep tissue imaging: prospects in redox imaging and disease diagnosis," J. Biomed. Opt. **10**(5), 051407 (2005).
19. P. J. Tadrous, J. Siegel, P. M. W. French, S. Shousha, N. Lalani, and G. W. H. Stamp, "Fluorescence lifetime imaging of unstained tissues: early results in human breast cancer," J. Pathol. **199**(3), 309–317 (2003).
20. M. W. Conklin, P. P. Provenzano, K. W. Eliceiri, R. Sullivan, and P. J. Keely, "Fluorescence lifetime imaging of endogenous fluorophores in histopathology sections reveals differences between normal and tumor epithelium in carcinoma in situ of the breast," Cell Biochem. Biophys. **53**(3), 145–157 (2009).
21. M. J. Koehler, A. Preller, P. Elsner, K. König, U. C. Hipler, and M. Kaatz, "Non-invasive evaluation of dermal elastosis by in vivo multiphoton tomography with autofluorescence lifetime measurements," Exp. Dermatol. **21**(1), 48–51 (2012).
22. P. P. Provenzano, C. T. Rueden, S. M. Trier, L. Yan, S. M. Ponik, D. R. Inman, P. J. Keely, and K. W. Eliceiri, "Nonlinear optical imaging and spectral-lifetime computational analysis of endogenous and exogenous fluorophores in breast cancer," J. Biomed. Opt. **13**(3), 031220 (2008).
23. W. Denk, J. H. Strickler, and W. W. Webb, "Two-photon laser scanning fluorescence microscopy," Science **248**(4951), 73–76 (1990).
24. D. L. Price, S. K. Chow, N. A. B. Maclean, H. Hakozaki, S. Peltier, M. E. Martone, and M. H. Ellisman, "High-resolution large-scale mosaic imaging using multiphoton microscopy to characterize transgenic mouse models of human neurological disorders," Neuroinformatics **4**, 65–80 (2006).
25. D. D. U. Li, J. Arlt, D. Tyndall, R. Walker, J. Richardson, D. Stoppa, E. Charbon, and R. K. Henderson, "Video-rate fluorescence lifetime imaging camera with CMOS single-photon avalanche diode arrays and high-speed imaging algorithm," J. Biomed. Opt. **16**(9), 096012 (2011).
26. R. Patalay, C. Talbot, Y. Alexandrov, I. Munro, M. A. Neil, K. König, P. M. French, A. Chu, G. W. Stamp, and C. Dunsby, "Quantification of cellular autofluorescence of human skin using multiphoton tomography and fluorescence lifetime imaging in two spectral detection channels," Biomed. Opt. Express **2**(12), 3295–3308 (2011).
27. R. Patalay, C. Talbot, Y. Alexandrov, M. O. Lenz, S. Kumar, S. Warren, I. Munro, M. A. Neil, K. König, P. M. W. French, A. Chu, G. W. H. Stamp, and C. Dunsby, "Multiphoton multispectral fluorescence lifetime tomography for the evaluation of basal cell carcinomas," PLoS One **7**(9), e43460 (2012).
28. J. McGinty, N. P. Galletly, C. Dunsby, I. Munro, D. S. Elson, J. Requejo-Isidro, P. Cohen, R. Ahmad, A. Forsyth, A. V. Thillainayagam, M. A. Neil, P. M. W. French, and G. W. Stamp, "Wide-field fluorescence lifetime imaging of cancer," Biomed. Opt. Express **1**(2), 627–640 (2010).
29. K. Dowling, M. J. Dayel, M. J. Lever, P. M. W. French, J. D. Hares, and A. K. Dymoke-Bradshaw, "Fluorescence lifetime imaging with picosecond resolution for biomedical applications," Opt. Lett. **23**(10), 810–812 (1998).
30. X. Y. Dow, S. Z. Sullivan, R. D. Muir, and G. J. Simpson, "Video-rate two-photon excited fluorescence lifetime imaging system with interleaved digitization," Opt. Lett. **40**(14), 3296–3299 (2015).
31. M. Hammer, D. Schweitzer, S. Richter, and E. Königsdörffer, "Sodium fluorescein as a retinal pH indicator?" Physiol. Meas. **26**(4), N9–N12 (2005).

## 1. Introduction

Cancer is the second leading cause of death in the United States and was responsible for 585,000 deaths in 2014 [1]. The standard of care for many types of cancer, including malignant tumors of the breast, is surgical resection of the tumor and additional surrounding normal tissue. Excised tissue is evaluated using conventional histological examination, however this requires a delay of up to one day for fixation, paraffin embedding, sectioning and staining [2]. This delay between initial surgery and pathological assessment may necessitate second surgery, should the surgical margin prove to be positive or insufficient on post-operative pathologic examination. Second surgeries pose additional risk to the patient, delay reconstructive procedures, may delay administration of adjuvant chemotherapy, and

#247756 Received 11 Aug 2015; revised 1 Oct 2015; accepted 1 Oct 2015; published 8 Oct 2015

incur financial burden on the healthcare system [3]. In order to minimize morbidity and improve cosmetic outcomes, it is important to reduce the rates of repeat surgeries while minimizing the amount of normal tissue excised around the tumor margin [4, 5]. Gross examination of resected specimens has limited sensitivity, with residual tumor present near the surgical margin in up to 40% of breast cancer patients on subsequent histology [6, 7]. Intraoperative microscopic pathologic examination (frozen section) improved detection of tumor at the margin in breast lumpectomy [8], but is challenging to use in breast specimens because of their high fat content. In addition, due to time constraints, only a limited number of frozen sections can be performed. Thus, improved imaging techniques for rapid assessment of surgical margins are needed.

Two-photon microscopy (TPM) has had a revolutionary impact on biological research by enabling rapid subcellular resolution imaging of thick, unfixed tissue with excellent contrast and depth sectioning [9, 10]. The high resolution of TPM combined with its molecular specificity makes it an excellent tool for visualizing morphologic features of the tissue, such nuclear size and texture as well as extracellular matrix and connective tissue fibers, changes in each of which are important hallmarks of neoplasm [11, 12]. However, while TPM can be performed with extrinsic contrast agents to label specific cellular or tissue components or even cellular receptors, these agents may interfere with subsequent histopathology, DNA testing or immunohistochemistry and are typically not approved for *in vivo* applications [13].

Fluorescent lifetime imaging microscopy (FLIM) is a related imaging modality that can image using intrinsic contrast. FLIM can be implemented using TPM for axial sectioning (TPM-FLIM) [14]. In FLIM, single or multiple photon excitation excites a fluorophore which decays with a characteristic time constant that depends on the specific fluorophore, pH, temperature, local proteins and other characteristics [15–18]. FLIM therefore provides extensive information on the microenvironment of individual cells or entire tissues which could reflect metabolic changes associated with malignancy [15]. TPM-FLIM has shown promise as a means of detecting pathology in preserved human breast specimens [19], breast cancer models [20] as well as dermatology imaging *in vivo* [21]. Recent results have also demonstrated sensitivity to mouse mammary tumors based on changes in lifetime, an exciting result that suggests applicability to human surgical guidence [20, 22].

However, because TPM and TPM-FLIM signals scale with the square of the excitation light intensity, both techniques can only be performed under high numerical aperture (NA), high magnification imaging [23]. Consequently, it is challenging to extend these techniques to the large fields of view required for analyzing surgical specimens. While high speed imaging and mosaicking of samples is an established technique for wide-area TPM imaging [24], to date TPM-FLIM has been limited to very small fields because of the extremely slow acquisition rates of existing TPM-FLIM systems which use time correlated single photon counting (TCSPC) [25–27]. It should be noted that FLIM without TPM can be implemented in a wide field geometry significantly faster than TCSPC [28, 29], but does not provide the depth sectioning required for imaging thick samples and suffers from relatively low imaging speed compared to TPM. Therefore, although FLIM has shown promise as a means for imaging and detecting cancer pathology, it has not been possible perform a systematic evaluation of TPM-FLIM in fresh surgical specimens and to assess its potential for intrasurgical evaluation.

To address these limitations, we have developed a new method of TPM-FLIM imaging using direct temporal sampling (DTS) of fluorescent decays phase-locked to a high harmonic of mode-locked laser repetition rate. With this method, we demonstrate measurement of intrinsic fluorescent lifetime in freshly-excised human breast specimens at a rate of over 7 megapixels per second after averaging. In contrast to TCSPC, which sacrifices throughput for exquisite sensitivity and temporal resolution, DTS-FLIM is designed to maximize throughput such that centimeter-scale samples can be rapidly imaged at cellular resolution. DTS-FLIM is related to the recently published work of Dow *et al*. [30], which synchronized a scanner and

#247756 Received 11 Aug 2015; revised 1 Oct 2015; accepted 1 Oct 2015; published 8 Oct 2015

fast digitizer to the repetition rate of a titanium:sapphire laser, and reconstructed lifetimes from multiple interleaved decays. However, rather than interleaved sampling and reconstruction in post-processing as shown in [30], we use direct temporal sampling by generating a high harmonic (22x) of the excitation laser as a sampling clock and capturing an entire fluorescent decay in a single time-resolved acquisition. By eliminating the need to perform interleaved sampling, DTS-FLIM can be performed with higher electronic bandwidth, less complex post-processing, and on existing TPM systems without the need for specialized scanning hardware.

## 2. Methods

### *2.1 System design*

A commercial two photon microscope (Thorlabs, Inc.) using an 8 kHz resonant scanner and an XLUMPFL20XW 1.0 numerical aperture objective (Olympus) was modified by replacing the standard digitizer with a high-speed digitizer with up to 4.0 GHz sample rate and 12 bit resolution (ATS-9370, Alazar Technologies) (Fig. 1). Illumination was provided by Ti:Sapphire laser (Chameleon, Coherent) operated at 760 nm with 140 fs pulses at a repetition rate of 80 MHz. Illumination power was limited to less than 30 mW (measured after the objective). Emission light from 380 nm (the wavelength of second harmonic generation, SHG) to 650 nm was detected via a dichroic filter. The excitation wavelength was chosen to excite intrinsic fluorophores such as NADH and lipids while avoiding excessively short SHG emission wavelengths.

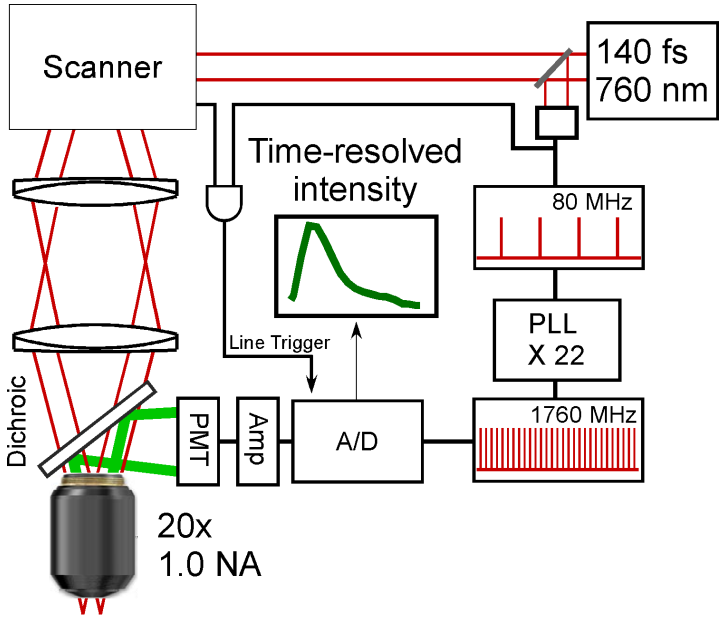


Fig. 1. DTS-FLIM system diagram. Femtosecond pulses are divided into sample (upper left) and reference arms (lower right). In the reference arm, a photodiode generates an electrical pulse train which is frequency multiplied 22-fold to 1.76 GHz and used as the sampling clock. In the sample arm, a resonant scanner and galvanometer image the tissue surface using a high NA objective. Fluorescent emission from the sample is split from the excitation via a 650 nm longpass dichroic filter and detected using a PMT with a further 650 nm short pass filter. Finally, direct time sampling (DTS) with 22 temporal bins per pixel is performed via the A/D.

A commercial phase locked loop (PLL, Analog Devices) was used to frequency multiply the output of a photodiode detecting the 80 MHz laser pulse train by 22-fold to generate a 1.76 GHz electrical pulse train which clocked the digitizer. A line trigger was provided by

#247756 Received 11 Aug 2015; revised 1 Oct 2015; accepted 1 Oct 2015; published 8 Oct 2015

edge doubling the 8 kHz (unidirectional) resonance scanner clock to generate a 16 kHz (bidirectional rate) signal, which was then passed through a high speed AND gate with the 80 MHz laser repetition rate. This configuration ensured that the start of each line begin synchronously with the laser pulses, greatly simplifying frame averaging. Detection was performed by a photomultiplier tube with a 570 ps rise time (Hamamatsu H10721-210) connected to an ACA-2 wideband amplifier (Becker & Hickl, GmbH). To mitigate RF pickup, the entire detector assembly was encased in aluminum and isolated from the environment with RF line filters.

Custom acquisition software written in c# (Microsoft, Inc.) was used to sample a 0.6 x 0.6 mm field at 2048 fluorescent excitations (linear axis) by 3584 excitations (resonant axis) at 22 samples per excitation in a total of 128 ms. Frames were then 8-fold coherently averaged and finally saved via solid state disk (SSD) array for a net rate of 7.3 megapixels per second at 568 ps sampling period. This real-time averaging step was essential for data reduction because the extremely high raw data rate (2.51 GB/s per channel) was impractical to stream to even a multi-SSD array in real-time. Following acquisition of each frame, and in parallel with data storage, a high-speed linear X-Y translation stage was used to translate the sample by a 350 micron increment, and acquire a new (partially overlapped) frame in a raster pattern. The total imaging time per frame was approximately 1.5 seconds, including saving and sample translation.

### *2.2 Sample preperation*

All studies were performed under an approved protocol from the Massachusetts Institute of Technology Committee on the Use of Humans as Experimental Subjects (COUHES) and the Beth Israel Deaconess Medical Center (BIDMC) Committee on Clinical Investigations (CCI). Histologically normal discarded and de-identified partial mastectomy specimens were obtained from the Department of Pathology at BIDMC shortly after resection and then transported to MIT in chilled RPMI solution. Samples were dissected to expose areas of interest and then placed in imaging cassettes bathed in chilled media during imaging to preserve intrinsic fluorophores.

### *2.3 Post-processing*

Frames were sequentially loaded and processed to produce lifetime coded images. Although deconvolution can be used to quantify precise fluorescence lifetimes, this process is computationally expensive, sensitive to noise, and depends on assumptions about fluorophore decay profiles that are difficult to know precisely for heterogeneous human tissue. However, for pathology imaging, quantifying the precise decay profiles of tissue samples is of secondary interest, and instead the objective is to qualitatively identify regions of pathology relative to normal tissue. To simplify processing, we have developed an efficient method of visualizing changes in lifetime based on the ratio of the long lifetime components to the total intensity. Our algorithm generates a color image in which the pixel intensity is determined by the overall fluorescence intensity, and the hue is determined by the ratio of intensity in the temporal bins from 1.7 to 5.1 ns divided by the total intensity. To visualize these ratios, pixels with 10% or lower energy at long lifetimes were colored fully saturated blue, with the hue increasing linearly towards red above 50% of total energy at long lifetimes. All images were processed using identical parameters and color scales. Following lifetime encoding, images were interpolated along the resonant axis to produce 2048x2048 isotropically sampled pixels. Finally, images were stitched and blended to produce large area mosaics using freely available photo stitching software (Image Composite Editor, Microsoft Research). As a result of image blending and correction for non-uniform sampling, the effective resolution of each mosaic was reduced by a factor 5, e.g. a 200 megapixel output mosaic required 1 gigapixel of individual frames.

#247756 Received 11 Aug 2015; revised 1 Oct 2015; accepted 1 Oct 2015; published 8 Oct 2015

## 3. Results

### *3.1 System validation*

The absolute accuracy of the DTS-FLIM system was determined using cuvettes of sodium fluorescein in phosphate buffered saline (PBS) at a concentration of 660 ng/ml. Following the measurement of instrument response function by removing the IR filter to enable direct femtosecond illumination of the PMT, and measurement of the laser repetition rate, deconvolution with an assumed single exponential decay yielded a lifetime of 4.11 ns (Fig. 2), an error of less than 1.5% from values reported previously by TCSPC [31]. The resulting instrument response function was found to have a 1.1 ns $e^{-1}$ fall time, and a 2.6 ns 90-10% fall time, with the longer 90-10% time largely due to weak oscilations in the instrument response function caused by the amplifer.

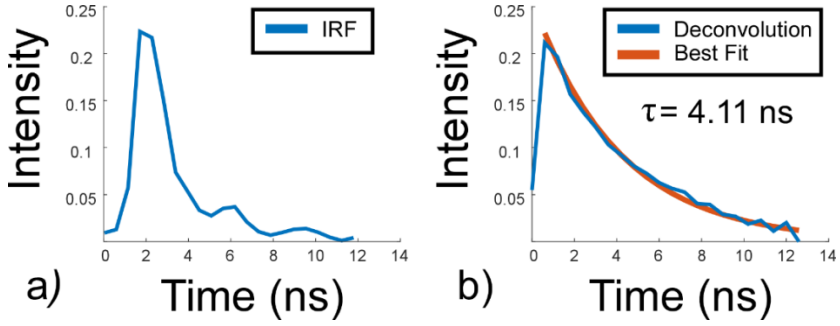


Fig. 2. Validation of the absolute accuracy of the direct temporal sampling TPM-FLIM system. a) System instrument response function. b) The deconvolved lifetime curve for sodium flouroscein in PBS together with the best single exponential fit.

### *3.2 Mastectomy imaging*

Histologically normal breast tissue collected from patients undergoing mastectomy at BIDMC without indication of cancer was imaged using DTS-FLIM. Regions with limited to moderate fat content were selected and then imaged to establish a baseline measurement of normal human breast tissue. Figure 3 shows a region of normal breast tissue with well-resolved regions of adipocytes, supporting stroma, and blood vessels. Lifetime ratios are ~0.2 in the relatively acellular stromal regions are with isolated strands of collagen having lifetime ratios as high as 0.3 distinctly visible. This low lifetime ratio is likely due to substantial contribution from second harmonic generation in collagen. Figure 4 shows a region surrounding a breast duct from a different mastectomy specimen. The lifetime ratio observed from surrounding stroma is in agreement with Fig. 3, while the breast duct shows elevated lifetime ratio (> 0.4) with clear nuclear shadowing, indicating a highly cellular duct.

## 4. Discussion

Fluorescent lifetime imaging is a promising modality for imaging live tissue because it provides metabolic and molecular contrast without the need for extrinsic agents. Preliminary studies have demonstrated exciting results in both small animal models and in human tissue, while the ability to provide molecular and metabolic contrast *in vivo* may enable imaging applications that are currently challenging using fluorescence intensity or elastic scattering imaging techniques. These include both *in vivo* imaging for applications such as surgical guidance, as well as the imaging of diagnostic specimens or biopsies that cannot be treated with contrast agents without compromising subsequent immunohistochemistry or DNA assays. However, in spite of these preliminary results, the application to human pathology remains unclear because of the limited TPM-FLIM field of view (10s to 100s of microns) versus typical histopathology and immunohistochemistry slides (10s of millimeters) has

#247756 Received 11 Aug 2015; revised 1 Oct 2015; accepted 1 Oct 2015; published 8 Oct 2015

prevented the examination of clinical specimens at the relevant spatial scales required to explore diagnostic potential. The development of techniques of that can enable evaluation of specimens large enough to be diagnostically useful is therefore an important step towards enabling clinical translation. The preliminary study presented in this work demonstrates, to the best of our knowledge, the first application of TPM-FLIM for imaging large, unfixed surgical specimens on a spatial scale comparable to conventional histopathology.

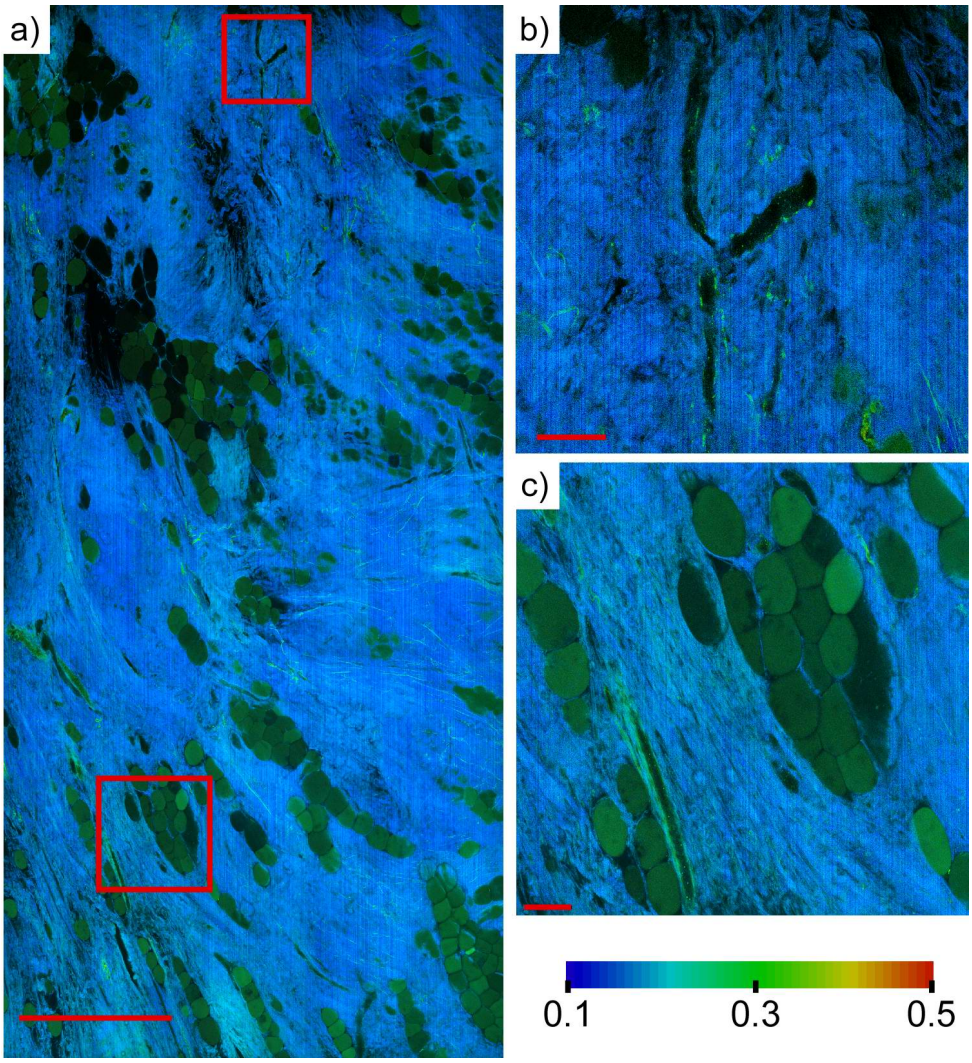


Fig. 3. a) 200 megapixel TPM-FLIM mosaic of an 4.0 x 6.8 mm field of view generated from 1 billion individual lifetime measurements in approximately 3 minutes. Differences in intrinsic lifetime clearly delineate adipocytes (green) from surrounding normal stroma (blue). Scale bar: 1 mm. b) Enlarged view of a branching blood vessel with epithelial cell lining. Scale bar: 100 um. c) Enlarged view of adipocytes and adjacent blood vessel (lower left). Scale bar: 100 um.

#247756 Received 11 Aug 2015; revised 1 Oct 2015; accepted 1 Oct 2015; published 8 Oct 2015

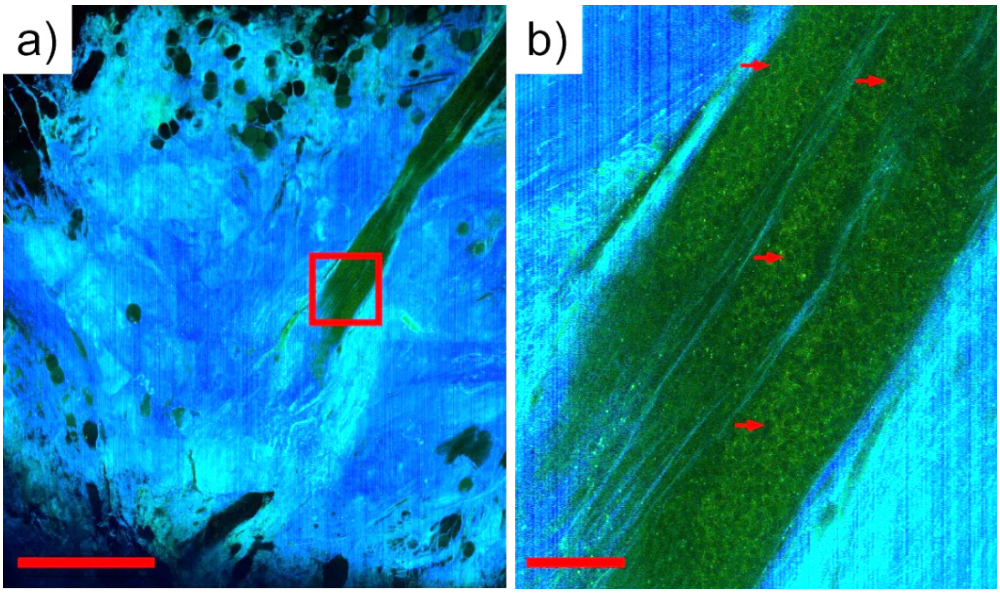


Fig. 4. a) TPM-FLIM mosaic of the region surrounding a breast duct. Scale bar: 1 mm. b) Enlarged view of the cellular region of a breast duct showing enhanced long lifetime component relative to surrounding stroma. Prominent nuclear shadows can be observed in the ductal region (arrows). Scale bar: 100 microns.

The key advance enabling these results is the development of direct temporal sampling FLIM, which enables simultaneous temporal binning of large numbers of photons in a single excitation event by phase-locking a detector to a high harmonic of the excitation rate. Since the analog bandwidth and sampling rate can be very high (up to 50 times the 80 MHz repetition rate for our A/D), the temporal resolution of a directly sampled waveform is limited only by the fall time of the optical detector. For typical large area PMTs, this is on the order of 1-2 nanoseconds. This figure can however be readily improved simply by using faster detectors such as hybrid PMTs or microchannel plate detectors, which potentially improve the temporal response several-fold. However, in our preliminary study, the temporal resolution appeared adequate to resolve different tissue components, at least in normal breast tissue. A more significant drawback in our implementation was the relatively high RF background noise and significant oscillation in the instrument response function introduced by using a 50 ohm impedance voltage amplifier to increase the very weak PMT currents for digitization. As a result of this noise, we were forced to average multiple excitations to improve SNR at the expense of imaging speed. The use of more suitable amplifiers may enable much more sensitive measurements as well as higher imaging speed.

In contrast to TCSPC, DTS-FLIM enables very high imaging speed at the expense of greatly reduced temporal resolution because photon counting cannot be employed. With the temporal resolution of the PMTs employed in this study, quantifying redox states using intrinsic contrast agents such as nicotinamide adenine dinucleotide (NADH) would be challenging. Furthermore, without photon counting, measurements are extremely sensitive to external interference making proper amplifier selection critical. At the same time, with increases in A/D bandwidths and sampling speeds such as those used in coherent telecommincations, we expect that higher time resolutions should become available in the future.

Finally, in this study, we observed consistent lifetime ratios for normal fat and stroma across specimens and within widely separated areas of the same specimen. Collagen lifetime was consistently less than adipocytes, which were consistently a little less than cellular areas of breast ducts and the linings of blood vessels. The increasing lifetime ratio with cellularity

#247756 Received 11 Aug 2015; revised 1 Oct 2015; accepted 1 Oct 2015; published 8 Oct 2015

may reflect both a reduction in SHG with increasing cellularity as well as additional longer lifetime metabolites in metabolicly active tissue. Our imaging results suggest that lifetimes of the fluorescent components of normal breast tissue are well regulated, and furthermore, that the lifetime ratio increases with cellularity. Future studies will be required to determine if the trend of increasing lifetime ratio extends to conditions such as carcinoma or carcinoma *in situ* that result in increased cellularity.

## 5. Conclusion

We have demonstrated the feasibility of imaging large human pathology samples using direct temporal sampling DTS-FLIM, imaging 4.0 mm x 6.8 mm fields of view within 3 minutes, orders of magnitude faster than previous methods. Using DTS-FLIM, we present what we believe are the highest resolution TPM-FLIM images generated in freshly-excised human tissue. We have developed a simple and computationally efficient visualization method based on the ratio of long lifetime fluorescence to total intensity that provides effective and reproducible contrast in mastectomy specimens. Preliminary results imaging breast surgical specimens suggests that lifetime ratio may be a useful method for evaluating surgical pathology.

## Acknowledgment

The authors thank Yuankai K. Tao, Ben Potsaid and Jeff Brooker for technical discussions and assistance. This study was supported in part by the National Institutes of Health R01-CA178636-02, R01-CA075289-17, F32-CA183400-02 and Air Force Office of Scientific Research AFOSR contracts FA9550-12-1-0551 and 15RT0913.

#247756 Received 11 Aug 2015; revised 1 Oct 2015; accepted 1 Oct 2015; published 8 Oct 2015